Research Article

Utilization of Carbon Monoxide as a Fuel: Economic Analysis and Reactor Design for Carbon Monoxide Oxidation Coupled with Heat Recuperation

Deep M. Patel[1,2] (ID)

[1]Department of Chemical Engineering, Nirma University, Sarkhej-Gandhinagar Highway, Ahmedabad, Gujarat, 382481, India
[2]Department of Chemical & Biological Engineering, Iowa State University, Ames, IA. 50014, United States of America
 Email: pateldeep7998@hotmail.com

Abstract: Carbon Monoxide is one of the unrequired and environmentally harmful by-products of various industries. A detailed design of process equipment for utilizing Carbon Monoxide as a fuel in industrial premises via Novel Zero Carbon Emission Process (NERS) is provided. A preliminary economic analysis of the designed system is also provided to enhance its practical viability. Based on economic evaluation, it is calculated that one can quickly achieve a temperature of around 523.15 K (250 °C) for water flowing at about 6 kg/s through the heat recuperation system installed in the process equipment. Hence a significant amount of energy that is otherwise wasted in the form of carbon emissions can be economically recovered (having an approximate payback period of around 1.5 years, based on economic analysis and reactor design as per bench-scale data available in the literature).

Keywords: heat recovery, bubbling fluidized-bed reactor, green energy, CO oxidation, sustainable energy

Notations

D_{FBR}	Diameter of Fluidized-Bed Reactor, m
H_{FBR}	Height of Fluidized-Bed Reactor, m
U_o	Feed inlet velocity, m/s
d_b	Bubble diameter, m
ε_{MF}	Bed-porosity at minimum fluidization velocity
U_{MF}	Minimum fluidization velocity, m/s
U_{br}	Relative bubble velocity, m/s
U_b	Bubble velocity, m/s
δ	Bed fraction in bubbles
α	Volume of wake to that of bubble
K_{BC}	Mass Transfer Coefficient for Bubble to Cloud mass transfer

K_{CE}	Mass Transfer Coefficient for Cloud to Emulsion mass transfer
f_b	Fraction of solid in bubble to that in bed
D	Diffusivity, m^2/s
ε_F	Bed-porosity at fluidization velocity
ε	Extent of reaction
f_c	Fraction of solid in cloud and wake to that in bed
f_e	Fraction of solid in the rest of emulsion to that in bed
ΔG	Gibbs Free Energy (J/mol)
INR	Indian Rupees (1 INR = 0.013 $)
RIL	Reliance Industries Limited
FBR	Fluidized Bed Reactor
$\%X_{CO}$	%Conversion of CO
W	Weight of Catalyst, kg
ASME	American Society of Mechanical Engineers
k'	Rate constant, $(m^3 gas)^n/[(mol\ A)^{n-1}(kg\ catal).s]$
k'''	Rate constant, $(m^3 gas)^n/[(mol\ A)^{n-1}(m^3\ catal).s]$
a	Activity of a catalyst
t	Time
T	Temperature
P	Pressure

1. Introduction

A significant increase in the air pollution index over the last few decades seems to have made a notable impact on global air quality, which has been deteriorating at a tremendous rate. An indirect impact of an increasing air pollution index is global warming, which is due to the majority of components like CO_x, NO_x and SO_x. In order to abate various negative impacts of global warming, a current Paris agreement[1] has been signed by various global leaders for maintaining the global temperature rise below 2 K. As per recent data,[2] Carbon dioxide is observed to contribute 30% to the overall increase in global temperature. Due to higher energy demand in 2018, global CO_2 emissions from the energy extraction sector increased by 1.7% to a historic high of 33.1 Gt CO_2. The power sector alone accounts for nearly two-thirds of the emissions growth. Coal used in power generation itself surpassed 10 Gt CO_2, mostly in Asia.[2] Therefore in order to curb the emission of noxious gases, various cogeneration approaches have been previously proposed, e.g., utilizing excess waste heat generated in gas turbines for local heat supply to alleviate the dependence on petroleum resources for heat generation.[5] Though such approaches might reduce CO_2 emissions up to a certain extent, they might not be sufficient to achieve the goal of zero emissions. Therefore, direct utilization of CO_2 to produce commodity chemicals like methanol, ethanol, formaldehyde, etc. through renewable electricity via an electrochemical route seems a relatively more feasible option.[3]

Carbon Monoxide is a poisonous greenhouse gas, which is a by-product of the incomplete combustion of hydrocarbons. In order to reduce Carbon Monoxide emissions, an additional oxidation step of CO to CO_2 is necessary for the complete utilization of waste carbon from industrial stack emissions to synthesize commodity chemicals. Recent efforts[4,5] to oxidize Carbon Monoxide occupy an important place in the literature since it contributes significantly to controlling air pollution, especially those from industrial stacks and automobiles. The majority of the researchers have investigated the oxidation of Carbon Monoxide at a laboratory scale[6-8] with an aim to reduce its contribution to environmental pollution, but no significant efforts have been made to implement such an idea at the industrial scale due to availability of only a few potential catalyst candidates with significant activity and higher stability. However, recently in our previous work,[9] we have provided a whole new pathway that channels the ongoing research to treat Carbon Monoxide as a potential heat source rather than a pollutant. Hence a Novel Zero Carbon Emission Process (NERS Process) was proposed, which utilizes carbon emissions to generate heat (thereby reducing a significant amount of load on fossil fuel to generate heat), along with the production of methanol. Due to reduction in reliability of fossil fuels, a

significant amount of carbon footprints of an industry can be reduced by adopting this process.

In the proposed NERS process,[9] after the separation of carbon dioxide in the first stage and removal of SO_X and NO_X in the second, the third stage (which is a critical part of the whole process) utilizes Carbon Monoxide as a fuel to generate a significant amount of heat (257.2 kJ/mol of CO) by oxidation of CO to CO_2, followed by CO_2 to methanol synthesis in the last stage. One of the significant drawbacks of our proposed idea was the unavailability of technology to economically extract the heat generated during this step. Therefore, in order to overcome this limitation, a detailed design of a bubbling fluidized-bed reactor along with an internal heat recuperation system is provided in order to oxidize Carbon Monoxide in the presence of air. By choosing the fluidized-bed reactor (FBR) over plug flow and mixed flow reactors, we are implicitly compromising the contacting efficiency due to its inherent problems of by-passing.[10] However since the extraction of heat generated during the exothermic reaction is quite easier as compared to other reactors, this design of reactor is preferred. The converted CO_2 from the designed FBR is further sent for the final stage of methanol production, as shown in our previous study.[9] We note that the current work is novel since we provide a detailed reactor design and techno-economic analysis of one of the key stages in our previously proposed NERS process.[9] Finally, this work is first of its kind to provide a detailed techno-economic analysis and reactor design for a CO oxidation coupled with heat-extraction in a single step. Such a study is a key step to potentially scale up the NERS process to the pilot scale.

The preliminary design data (required for pilot plant set-up) predicted in this article are within an accuracy range of ± 30% due to various assumptions provided in corresponding design theories and models. The proposed design is based on stack emission data of Reliance Industries Limited, Jamnagar, Gujarat, INDIA; thus, actual design parameters may vary from industry to industry, based on their stack emission data and environmental conditions.

2. Methodology

We note that the metrics for the thermal stability of a catalyst used in this study is time till which it can maintain steady-state conversion and turnover frequency at respective reaction conditions.[11] The design of the Bubbling-Fluidized Bed Reactor is carried out by correlations presented by Davidson's theory for bubble-cloud circulation and Higbie's theory for cloud-emulsion diffusion.[10] The thickness of the reactor material is calculated via correlations provided in ASME section VIII. The catalyst[11] assumed to be used in the proposed FBR design is NiO(Ga)(250) due to its high equilibrium conversion (~ 70%), high thermal stability (> 2 hours for 50 mg catalyst, 3 torr of stoichiometric mixture of $CO + 0.5 * O_2$ at 303.15 K), and ease of availability of required kinetic data as compared to other potential catalysts, as listed in our previous work.[9]

2.1 *Assumptions*

While developing the design of FBR with an internal heat recuperation system, we have made the following assumptions. We note that a few of the assumptions for this study were made based on the author's experience with reactor designing for solid/gas systems.

- The gas flow through the cloud is negligible since the volume of the cloud is quite insignificant for fast moving bubbles.
- The gas flow (either up or down) through the emulsion is negligible since this flow is quite smaller as compared to the flow through bubbles.
- CO and air form an ideal gas mixture.
- Extent of Catalyst deactivation is negligible compared to extent of CO oxidation, i.e., NiO(Ga)(250) is experimentally observed to reach that steady-state conversion for > 4 hours, which is greater than timescale to reach steady-state conversion for CO oxidation on NiO(Ga)(250), i.e., ~ 1.5 hours.[11]
- Reactions occurring on the surface of the catalysts are elementary.
- Concentrations of O^-, Ni^{3+} and Ni^{2+} ions are constant.
- Inlet feed velocity (U_o) is 0.6 m/s.
- The diameter of the FBR (D_{FBR}) is 2 meters.

- Cornelius theory[12] is applicable for determining bubble diameter, with parameter 'c' equal to zero (for safety reasons).
- The value of Diffusivity coefficient (D) for mass transfer between emulsion and cloud is of the order of $2*10^{-5}$ m²/s.
- The value of constant ' ' is 0.33.[10]
- The value of the ratio of the volume of solids in bubble to the volume of bed (f_b) is 0.001.[10]
- The inlet temperature of water in the internal heat recuperation system and that of inlet feed gas to FBR is 298.15 K.
- The heat generation rate is assumed to be constant within the heat recuperation system. (Refer the following section for more detail)
- Required conversion of Carbon Monoxide is 99.99%.

3. Designing and technical analysis

Fluidized-Bed reactors are practically classified into four categories based on their regime of operation:
1. Bubbling fluidized-bed reactor
2. Turbulent fluidized-bed reactor
3. Flow-through fluidized-bed reactor
4. Pneumatic conveying fluidized-bed reactor

Table 1. Physical properties of feed inlet (Carbon Monoxide and Air) and catalyst used in bubbling fluidized-bed reactor.

Carbon Monoxide	
Dynamic viscosity, Pa.s	1.7633×10^{-5}
Density, kg m⁻³	1.14
Specific Heat Capacity (C_p), kJ/kg K	1.040
Air	
Dynamic viscosity, Pa.s	1.82325×10^{-5}
Density, kg m⁻³	1.2754
Specific Heat Capacity (C_p), kJ/kg K	1
Inlet CO-Air mixture	
Dynamic viscosity, Pa.s	1.8371×10^{-5}
Density, kg m⁻³	1.24421
Specific Heat Capacity (C_p), kJ/kg K	1.0095
NiO(Ga)(250) catalyst	
Assumed average Particle size, μm	60
Assumed solid Density, kg m⁻³	1200

A bubbling fluidized-bed reactor was selected, because the catalyst sample stays suspended in the gas stream, which facilitates uniform temperature distribution across the catalyst particles, and thereby avoiding the creation of hotspots, which might be the case for flow-through and pneumatic conveying fluidized-bed reactors. Turbulent FBR was avoided because, in the turbulent regime of inlet feed, the contact surface area between catalyst particle and gas reduces. High contact surface area at gas-solid interface is extremely critical for efficiently extracting the heat generated through CO oxidation at the solid-gas interface. A detailed discussion of all the above four categories of FBR is provided elsewhere.[10,13]

The designed reactor is assumed to have an inlet of CO at 9.1 kg/hr (based on technical analysis of stack emission data of RIL in our previous article[9]) and air at 30 kg/h (1.5 times in excess than stoichiometric requirement for CO oxidation). The feed inlet and outlet temperatures are assumed to be 298.15 K, which is a normal room temperature at Jamnagar, Gujarat, INDIA. Table 1 summarizes all the physical properties of an inlet stream and catalyst used.

3.1 *Rate kinetics of oxidation of Carbon Monoxide*

Based on the data available in literature,[11] an experimental plot of conversion in terms of % moles of CO reacted ($\%X_{CO}$) vs. time for oxidation of CO on NiO(Ga)(250) in a static reactor is shown in Figure 1. Note that conversion vs. time profile depends only on the catalyst and the chemical reaction and is independent of the reactor choice.
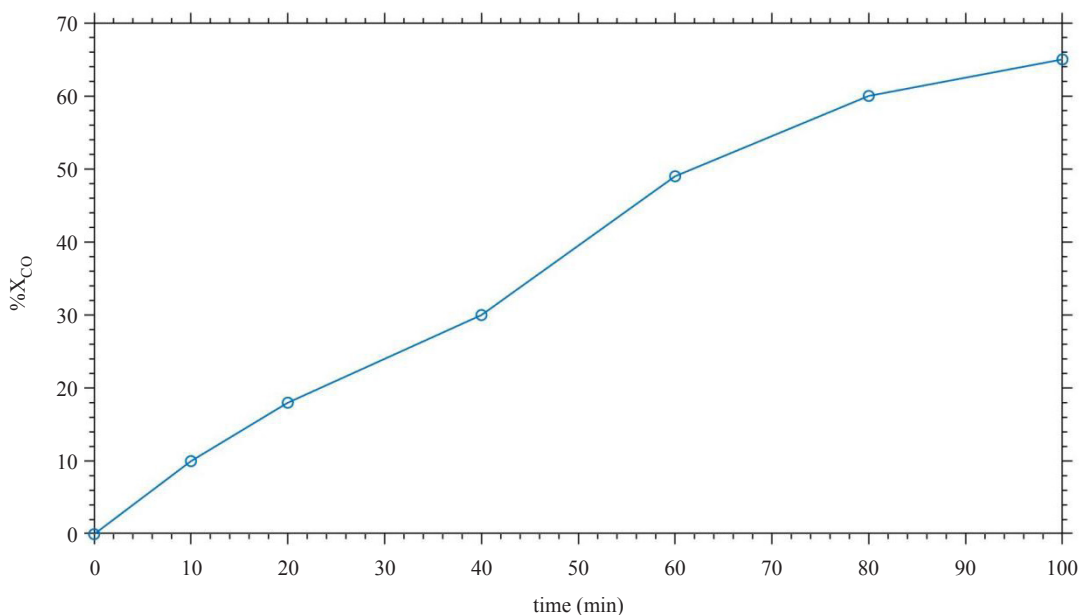
Figure 1. Conversion (%) vs. time plot for oxidation of Carbon Monoxide over NiO(Ga)(250) based on data available in the literature.[11]

Reaction mechanism for *CO* oxidation on NiO(Ga)(250) is described in Rxn(1) and Rxn(2), based on literature.[11]

$$0.5O_2 + Ni^{2+} \rightarrow O^-_{(ads)} + Ni^{3+} \qquad\qquad \text{Rxn(1)}$$

$$O^-_{(ads)} + CO + Ni^{3+} \rightarrow CO_2 + Ni^{2+} \ (\text{Rate limiting}) \qquad\qquad \text{Rxn(2)}$$
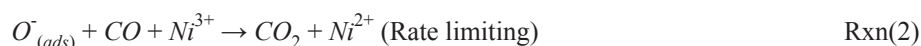
According to a detailed discussion,[11] the slowest step for oxidation of Carbon Monoxide on NiO(Ga)(250) is an interaction between adsorbed Carbon Monoxide and oxygen molecule, i.e. Rxn(2). Assuming that Ni^{2+} sites are available in abundance on the surface of a catalyst, we can state that the concentration of Ni^{2+} and Ni^{3+} sites remain

constant (according to Rxn(1)). Also, since oxygen was provided in excess (as compared to *CO*) while studying the surface phenomena,[7] the concentration of O^- ions can also be stated as constant. Assuming the elementary nature of Rxn(2) (based on the detailed arguments provided in literature[8]), the reaction rate can be given by (1),

$$-rCO = a * k' * CCO \qquad (1)$$

$\because$ a = activity of the catalyst

k' = rate constant, (kg catal)$^{-1}$s^{-1}

C_{CO} = Concentration of Carbon Monoxide, mol m^{-3}

Based on discussion provided in Appendix A, the deactivation rate of a catalyst can be given by (2).

$$-\frac{da}{dt} = a^1 C_{O_2} + C_{O_2}^2 \qquad (2)$$

Now, (1) can be written as (3).

$$(1/W) * \frac{dC_{CO}}{dt} ak'C_{CO} \qquad (3)$$

$$\therefore C_{CO(initial)} * \frac{dX_{CO}}{dt} = W * a * k' * C_{CO(initial)} * (1/X_{CO}) \qquad (4)$$

Eliminating $C_{CO(initial)}$ from both sides of (4),

$$\frac{dX_{CO}}{(1-X_{CO})} = W * a * k' * dt \qquad (5)$$

Integrating (5) within limits of conversion from 0 to X_{CO} and that of corresponding time from 0 to *t*, we get (6):

$$\ln(1-X_{CO}) = -W * a * k' * t \qquad (6)$$

Based on the experimental data[7] as plotted in Figure 1, and further plotting $\ln(1 - X_{CO})$ vs. time in Figure 2, it is observed that the value of $(a * W * k')$ is -0.0107681342 (m^3 gas/min) with R^2 value of 0.99601.

Since *W* is 50 mg (weight of catalyst taken during experimentation[11]) and assuming that the change in the activity is negligible (since the operational temperature is 298.15 K and due to excess air supply, *CO* poisoning is insignificant), the value of $(a * k')$ would be 3.5893 m^3 gas. sec^{-1}. (kg catalyst)$^{-1}$. Thus, the value of $(a.k''')$ would be 4307.2 m^3 (gas) sec^{-1}. (m^3 catalyst)$^{-1}$.
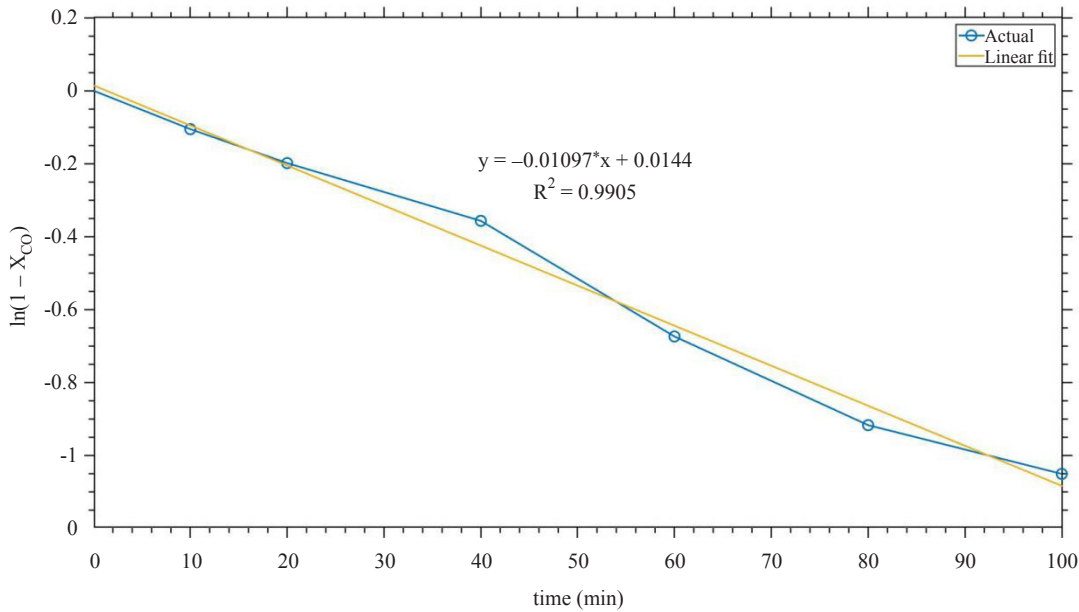
Figure 2. $\ln(1 - X_{CO})$ vs. time plot for oxidation of CO over NiO(Ga)(250) based on data available in literature.[11]

3.2 Design aspects of bubbling FBR for oxidation of Carbon Monoxide

The reactor's dimensional details provided hereby are based on various equations proposed by Davidson's and Higbie's theory, whereas mechanical details are based on equations provided by ASME section VIII. Also, plenum height is found via equations available in recent work.[9] Further, grid plate is recommended as a distributor due to its low cost, and corresponding dimensions are also calculated.

The velocity of a single bubble rising through a bed can be calculated via (7):

$$u_{br} = 0.711 * (g * d_b)^{0.5} \tag{7}$$

Therefore, the rise velocity of bubbles in a bubbling bed can be given as (8):

$$u_b = u_0 - u_{mf} + u_{br} \tag{8}$$

Further the bed fraction in bubbles can be evaluated via (9):

$$\delta = \frac{u_0 - u_{mf}}{u_b} \tag{9}$$

The down flow of emulsion solids (u_s) and rise velocity of emulsion gas (u_e) is evaluated by an approach provided in literature.[2] The mass interchange constant for mass transfer between bubble and cloud (K_{bc}), and for that between cloud and emulsion (K_{ce}) is evaluated based on (10) and (11), extracted from Davidson's theory:

$$K_{bc} = 4.50 * \left(\frac{u_{mf}}{d_b} \right) + 5.58 * \left(\frac{D^{0.5} * g^{0.25}}{d_b^{1.25}} \right) \tag{10}$$

$$K_{ce} = 6.77 * \left(\frac{\varepsilon_{mf} * D * u_{br}}{d_b^3} \right)^{0.5}$$ (11)

Here, the assumed value for the ratio of the volume of solid in bubble to volume of bed (f_b) is equal to 0.001, and thereby further two ratios, i.e. ratio of volume of solid in cloud and wake to the volume of bed (f_c), and the ratio of the volume of solids in rest of the emulsions to the volume of bed (f_e) are calculated via correlations provided in literature.[2] Therefore, the total fraction of solid fluidized (f_{total}) is calculated by summation of all the three ratios, which will be equal to ($1 - \epsilon_f$). Further, the expression for first order reactions in Bubbling FBR can be given by (12):[15]

$$\ln(\frac{1+\varepsilon}{1-X_A}) = \frac{\left[f_b k''' + \dfrac{1}{\dfrac{1}{\delta * K_{bc}} + \dfrac{1}{f_c k''' + \dfrac{1}{\dfrac{1}{\delta * K_{ce}} + \dfrac{1}{f_e k'''}}}} \right]}{f_{total}} * \frac{f_{total} * H_{fbr}}{u_0}$$ (12)

Here Height of FBR (H_{FBR}) is given by (13):

$$H_{fbr} = \frac{W}{\rho_c * A * (1 - \varepsilon_f)}$$ (13)

The value of bed porosity (ϵ_{mf}) at minimum fluidization velocity (u_{mf}) is calculated to be around 0.55 via general solid-fluid operation equation available in literature.[10] Simultaneously the value of heat generated within FBR, which is recoverable, is calculated by (14):

$$Q_{gen} = f_{total} * W * k' * \frac{C_{CO^*}(1 - X_{CO})}{(1 + \varepsilon)} * \Delta G$$ (14)

Further it is assumed that the cold fluid (water) is entering the pipeline made up of CuproNickel (having 16 mm ID and 20 mm OD) at 298.15 K and is required in the outlet at 473.15 K. Hence corresponding flow rate (refer to Table 2) is calculated from basic heat balance equations. The height of the Plenum is calculated by (15),[10] where the diameter of feedline is estimated via continuity equation to be 0.137 m, and the diameter of Plenum is taken to be the same as that of reactor vessel, i.e., 2 m with horizontal gaseous feed entry from the bottom of the vessel.

$$H_{plenum} = 0.2 * D_{plenum} + 0.5 * D_{feed}$$ (15)

Table 2. Summary of calculated final design parameters for bubbling fluidized bed reactor for CO oxidation coupled with heat extraction (as shown in Figure 3).

Parameters	Values
Assumed inlet stream velocity U_0 (m/s)	0.6
ϵ_{mf}	0.55
U_{mf}, m/s	0.019
Bubble diameter d_b, m	0.76
Assumed FBR diameter D_{FBR}, m	2
U_{br}, m/s	1.9404
U_b, m/s	2.5219
δ	0.23038
U_s, m/s	0.27643
U_e, m/s	-0.24188
K_{bc}, s^{-1}	0.118
K_{ce}, s^{-1}	0.05
f_b	0.001
f_c	0.03985
f_e	0.305479
ϵ_f	0.653671
H_{FBR} (calculated), m	1.81
H_{FBR} (Actual, assuming safety factor of around 3), m	5
Q_{gen}, kJ/s	2157.381
Assumed inlet water temperature $T_{water(i)}$, K	298.15
Required outlet water temperature $T_{water(o)}$, K	473.15
Calculated flowrate of water, kg/s	5.9
Feed pipe diameter, m	0.137
Plenum height, m	0.4685
Catalyst bed height, m	0.5308
Max. height (calculated from the base of catalyst bed) up to which pipelines for heat recovery can be installed, in meter	1.4
Pipeline Passes	1

Table 2. (cont.)

Parameters	Values
Pipeline arrangement	Horizontal (1.4 m above catalyst bed)
Pressure drop across the catalyst bed, Pa	2808.99
Pressure drop across the distributor, Pa	842.7
Hole diameter of distributor (grid), μm	37
Number of holes in distributor	280960
Wall thickness of reactor, mm	0.8
Welding efficiency	0.85
MOC of reactor	Stainless Steel (SS 316)
Max. stress (Yield) of SS 316, in MPa	500
Design Pressure, atm	3
Operating Pressure, atm	1

*Note: Here, meter(s) is denoted by 'm', atmosphere by 'atm', second(s) by 's', kilo(s) by 'k', Joule(s) by 'J', Pascal by 'Pa', micron(s) by 'μ', and millimeter(s) by 'mm'. Refer the notations provided in the beginning of the article for others.

Due to its low cost compared to other distributors like bubble caps and flat plates with holes, the grids are recommended to be used for supporting catalyst bed and distributing the incoming gaseous feed through it for fluidization purposes. The pressure drops across the catalyst bed and the distributor grid is evaluated by (16) and (17) respectively:[10]

$$\Delta P_b = \rho_g * g * h_{catalyst} * (1 - X_{CO}) \qquad (16)$$

$$\Delta P_b = 0.3 * \Delta P_b \qquad (17)$$

Since the average diameter of catalyst particles is 60 μm, the diameter of grid opening must be well beyond it. Based on the data available in literature,[9] the possible grid opening must be 37 μm. The velocity of gaseous feed through grid opening is evaluated by (18).[13]

$$U_h = C_d * \sqrt{\frac{2 * \Delta P_b}{\rho_g}} \qquad (18)$$

Now since the inlet feed flow rate is around 32 m³/hr, the number of openings required in the grid is calculated based on a simple continuity equation. Further, the reactor shell thickness is calculated based on ASME section VIII, with a safety factor equal to 3, and design pressure equal to 2 atm. The calculated values of all the design parameters are summarized in Table 2. A final depiction of the designed FBR is shown in Figure 3.

The material of construction is chosen SS 316 because it is the only economically available material[5] which is resistant to fume gases containing nitrogen, carbon and sulfur oxides along with certain hydrocarbon impurities. The composition of SS 316 is shown in Table 3.

Outlet Pipe

5 m

2 m

0.9 m
(Space for pipeline installation
for heat recovery)

0.5308 m
Catalyst bed

0.4685 m

Feed Pipe

Vessel: Fluidized Bed Reactor
Vessel MOC: Stainless Steel 316
Catalyst: Nio(Ga)(250)
Temperature: 298.15 K
Operating Pressure: 1-1.5 atm
Design Pressure: 3 atm
Reactor Wall Thickness: 0.8 mm
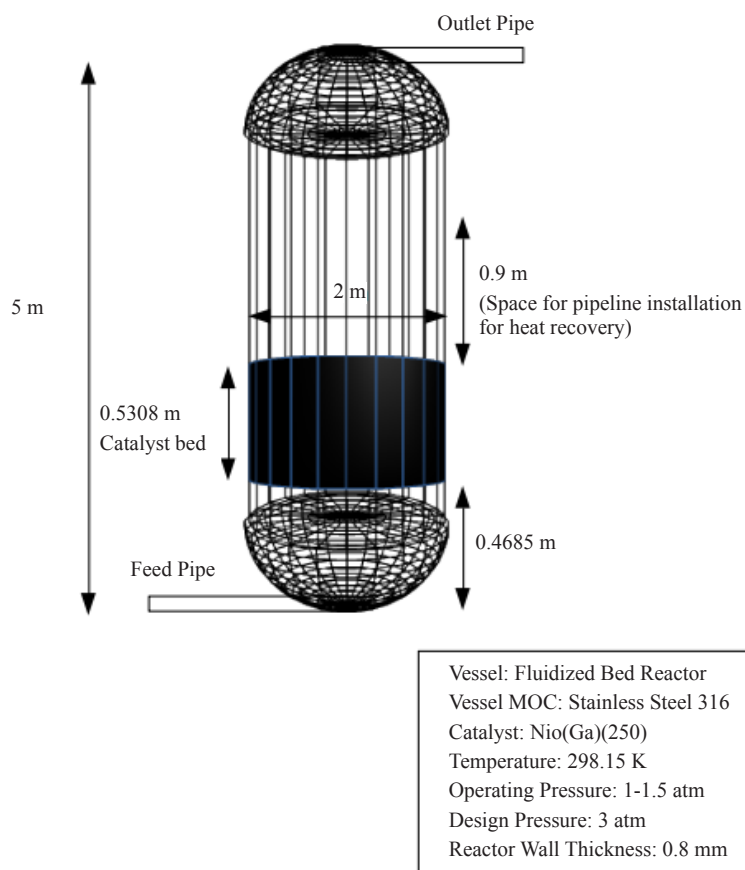
Figure 3. Estimated bubbling fluidized bed reactor design for heat recovery step of NERS process. Here, meter(s) is denoted by 'm', and atmosphere by 'atm'. Refer the notations provided in the beginning of the article for others.

Table 3. Composition[16] of Stainless Steel 316 in terms of weight percentage (%wt) of respective elements.

Elements	Composition (%wt)
Chromium	16.5-18.5
Nickel	10-13
Molybdenum	2-2.5
Manganese	0-2
Silicon	0-1
Nitrogen	0-0.11
Carbon	0-0.07
Phosphorous	0-0.05
Sulfur	0-0.03
Iron	Balance

4. Economic analysis

In our previous article,[9] a preliminary economic analysis is provided for the entire NERS process. However, in this article, an important step towards a detailed economic analysis is taken by thoroughly investigating the economic aspect of a particular stage of the proposed process from a designer's point of view. All the data provided hereby are based on the current market value available at corresponding public platforms. The actual price may vary based on freight charges and taxes imposed at the desired location of delivery.

According to the dimensions provided in the previous section, the quantity of SS 316 sheet required for the construction of the whole vessel is estimated to be around 0.03 m^3 or 300 kg. Since the cost of SS 316 in India is around 255 INR per kg,[9] the total cost of vessel material would be around 61,200 INR. Further, the costs of valves (assuming 3 valves are required, i.e., one safety valve and two flow control valves), contingency costs (assuming 10% of total cost[16]), construction cost (assuming 25% of the total cost[16]), paint (2.7% of the total cost[16]) and pipelines (8% of the total cost[16]) are summarized in Table 4.

Table 4. Analysis of fixed cost (in Indian Rupees (INR)) involved in CO oxidation combined with heat recuperation stage of NERS process.

Entities	Cost (INR)
Material of Construction	61,200
Wire Mesh support	45,000
Manufacturing Cost (25%)	185,495
Safety Valve[16]	8,000
Total cost of an inlet and an outlet valve[16]	10,000
Paint (2.7%)	15,174
Contingency costs (10%)	56,200
Pipeline (8%)	44,960
Miscellaneous (7.2%)	40,464
Margin to total fixed cost (25%)	140,498
TOTAL	561,991

*Note: All the percentage in the brackets denotes the contribution of respective entities to the total fixed cost. Current value of INR: 1 INR = 0.013 USD.

Since inlet gas is required at the speed of 0.6 m/s which shall be easily achieved by reducing the feed pipe inlet diameter to 0.14 m, no additional cost of a compressor is required for this stage of the proposed NERS process. The estimated cost of wire mesh with a 37-micron grid opening and 2 m diameter (since it is to be fitted in designed FBR having 2 m diameter for supporting catalyst) is around 45,000 INR in the market.[17] Therefore the total asset value would be 561,991 INR. Assuming that the service life of this vessel is 20 years as per the rules of Income Tax Department of India and taking its scrap value to be 0 INR, the total depreciation estimated is around 28,100 INR, based on linear depreciation accounting method. This method of accounting depreciation is used because it is one of the most common methods which is preferred by design engineers for the estimation of preliminary cost data.[2]

The total amount of heat generated in this process is 2,157.381 kJ/s, which is equal to $6.524 * 10^{10}$ J per annum

(assuming that FBR works continuously for 350 days out of 365 days). Since the majority of modern refineries (including RIL) are using low-volatile Bituminous coal to produce the same amount of heat prior to implementation of the proposed process, based on its calorific value, approximately 4,100 kg of low-volatile Bituminous coal will be saved. Simultaneously corresponding carbon and sulfur oxides will also be eliminated along with that from other units of refineries. Therefore, RIL would be saving around 40,000 INR per year (including cost of coal, its transportation cost and carbon tax[2]). Apart from the overhead costs like salaries of operators and workers (which is generally negligible when a single stage is considered from a huge complex refinery like RIL), there won't be any operational cost associated with this stage of the NERS process. Thus, there won't be any variable cost involved in this step of NERS apart from maintenance costs. Also, since NiO catalyst is already being used in the hydrogenation step in RIL refinery, there won't be any replacement cost for the deactivated catalyst due to the availability of the same within the industrial premises. An overall economic analysis of this stage is summarized in Table 5 based on the above arguments. Further, cumulative cash position chart based on data from Table 5 is plotted in Figure 4, assuming that extra land for supplementing the proposed process within the existing facility is already available and hence no extra land needs to be purchased. It clearly shows that within 1.5 years, the initial investment will be fully paid and make a profit.

Table 5. Overall economic analysis of the CO oxidation combined with heat recovery stage of the NERS process.

Entities	Cost (INR)
Fixed Cost	561,991
Depreciation per year	28,100
*Variable Cost per year (only Maintenance cost)	1,600
Revenue Generated per year	40,000

*Around 4% of the net income16
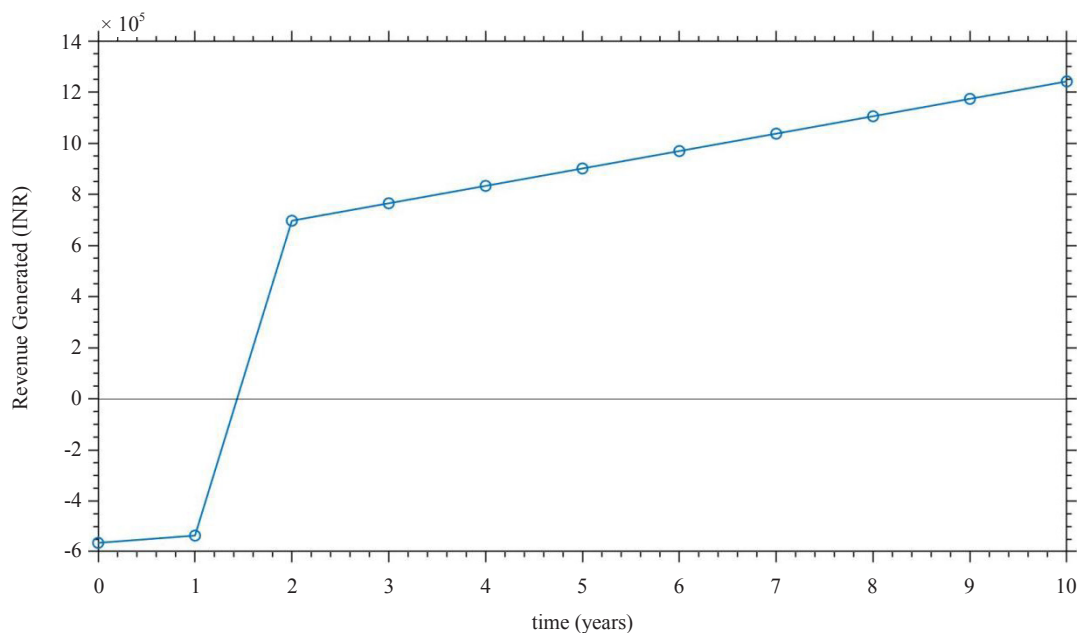
Figure 4. Cumulative Cash Position diagram of heat recuperation step of NERS process. (INR: Indian Rupees) Current value of INR: 1 INR = 0.013 USD.

Based on the economic data provided hereby, the process seems quite feasible from an industrial point of view. Additionally, if the profit earned by gaining carbon credits (since significant CO and CO_2 are being captured and utilized within the industrial premise) would have been accounted for, the payback period would have been way beyond 10 years.[2] Therefore it is coherent to say that implementing the NERS process for carbon sequestration inherently provides a perquisite of simultaneously reducing a significant load on boilers, along with economic savings. We again note that the techno-economic analysis provided in this work is only for CO oxidation coupled with heat recuperation stage. The CO_2 produced at the end of this stage could be converted to methanol or other commodity chemicals. A detailed accounting of the overall economics for CO_2 to methanol production is provided elsewhere.[9]

5. Direction for future research

The discussion and arguments provided in this work are based on an empirical reactor design scheme and preliminary techno-economic analysis, based on experimental data available in the literature.[11] In order to increase the confidence for potential scale-up of NERS process to a pilot scale, detailed studies must be required to understand: (i) the effect of feed composition on catalyst performance and heat recuperation rate, (ii) catalyst deactivation mechanism in the presence of poisons like SO_x, NO_x, elemental sulfur, and C1-C4 hydrocarbon species (majorly alkanes, and alkenes) as they are known to be present in the stack emissions of petroleum industries, (iii) detailed performance testing of commercially available carbon-capture technologies, and (iv) detailed performance testing of commercially available techniques for SO_x and NO_x separation from CO_x.

6. Conclusion

The article cogently presents the design and economic aspect of a heat recovery step of NERS process which utilizes Carbon Monoxide as a potential heat generator. A further refinement of the previously provided economic analysis is provided hereby, which concludes that the heat recovery step seems economically feasible in the long run. Based on the given techno-economic analysis of this stage, the heat recovery stage seems economically and environmentally favorable, but before implementing this step at industrial scale, a detailed pilot plant study must be carried out in order to make a detailed and accurate prediction of operating conditions, final reactor dimensions and economic data. Since all the carbon emissions are being used up for extraction of heat and production of methanol, one may expect zero carbon emission and a hence significant reduction in global temperature rise after the implementation of the proposed NERS process.

Conflict of interest

The author declares that he has no known competing financial interests or personal relationships that could have appeared to influence the work reported in this paper.

References

[1] The Paris Agreement. UNFCCC. https://unfccc.int/process-and-meetings/the-paris-agreement/the-paris-agreement (accessed Dec 12, 2019).
[2] IEA. Emissions. *Global Energy & CO₂ Status Report 2019*. https://www.iea.org/reports/global-energy-co2-status-report-2019/emissions#abstract (accessed Dec 11, 2019).
[3] Nitopi, S.; Bertheussen, E.; Scott, S. B.; Liu, X.; Engstfeld, A. K.; Horch, S.; Seger, B.; Stephens, I. E. L.; Chan, K.; Hahn, C.; Nørskov, J. K.; Jaramillo, T. F.; Chorkendorff, I. Progress and Perspectives on Electrochemical CO₂ Reduction on Copper in Aqueous Electrolyte. *Chem. Rev.* **2022,** *119*, 7610-7672.
[4] Aniz, C. U.; Nair, T. D. R. A Study on Catalysis by Ferrospinels for Preventing Atmospheric Pollution from Carbon

Monoxide. *Open Journal of Physical Chemistry*. **2011,** *1*, 124-130.

[5]   Mobini, S.; Meshkani, F.; Rezaei, M. Supported Mn Catalysts and the Role of Different Supports in the Catalytic Oxidation of Carbon Monoxide. *Chemical Engineering Science*. **2019,** *197*, 37-51.

[6]   Schiller, F.; Ilyn, M.; Pérez-Dieste, V.; Escudero, C.; Huck-Iriart, C.; del Arbol, N. R.; Hagman, B.; Merte, L. R.; Bertram, F.; Shipilin, M.; Blomberg, S.; Gustafson, J.; Lundgren, E.; Ortega, J. E. Catalytic Oxidation of Carbon Monoxide on a Curved Pd Crystal: Spatial Variation of Active and Poisoning Phases in Stationary Conditions. *J. Am. Chem. Soc.* **2018,** *140*, 16245-16252.

[7]   Yoshida, T.; Murayama, T.; Sakaguchi, N.; Okumura, M.; Ishida, T.; Haruta, M. Carbon Monoxide Oxidation by Polyoxometalate-Supported Gold Nanoparticulate Catalysts: Activity, Stability, and Temperature-Dependent Activation Properties. *Angewandte Chemie*. **2018,** *57*, 1523-1527.

[8]   Zhang, R.; Lu, K.; Zong, L.; Tong, S.; Wang, X.; Zhou, J.; Lu, Z.-H.; Feng, G. Control Synthesis of CeO_2 Nanomaterials Supported Gold for Catalytic Oxidation of Carbon Monoxide. *Molecular Catalysis*. **2017,** *442*, 173-180.

[9]   Patel, D. M.; Kodgire, P.; Dwivedi, A. H. Low Temperature Oxidation of Carbon Monoxide for Heat Recuperation: A Green Approach for Energy Production and a Catalytic Review. *Journal of Cleaner Production*. **2019,** *245*, 118838.

[10] Levenspiel, O. *Chemical Reaction Engineering*; Wiley India, 2007.

[11] El Shobaky, G.; Gravelle, P. C.; Teichner, S. J. Influence of the Surface Structure of a Nickel Oxide Catalyst on the Mechanism of the Room-Temperature Oxidation of Carbon Monoxide. *Journal of Catalysis*. **1969,** *14*, 4-22.

[12] Agu, C. E.; Pfeifer, C.; Eikeland, M. Tokheim, L.-A.; Moldestad, B. M. E. Models for Predicting Average Bubble Diameter and Volumetric Bubble Flux in Deep Fluidized Beds. *Industrial & Engineering Chemistry Research*. **2018,** *57*, 2658-2669.

[13] Kunii, D.; Octave L. *Fluidization Engineering*; Elsevier, 2012.

[14] Abdelgawad, B. *Design of a Gas-Solid Fluidized Bed Reactor at High Temperature and High Pressure*; Master's thesis, École Polytechnique de Montréal, 2014.

[15] Fogler, S. H. *Elements of Chemical Reaction Engineering*; Prentice Hall, 2019.

[16] Peters, M.; Timmerhaus, K.; West, R.; Peters, M. *Plant Design and Economics for Chemical Engineers*; McGraw-Hill, 2006.

[17] Abdelgawad, B. *Design of a Gas-Solid Fluidized Bed Reactor at High Temperature and High Pressure*; Master's thesis, École Polytechnique de Montréal, 2014.

Appendix A: Decay rate mechanism of NiO(La)(250) catalyst during oxidation of Carbon Monoxide

Based on a detailed argument available in literature[13], LH mechanism for the surface deactivation of a given catalyst can be summarized by Rxn(A1) to Rxn(A4):

$$CO_{(g)} \rightarrow CO_{(ads)} \qquad\qquad \text{Rxn(A1)}$$

$$CO_{(ads)} + Ni^{2+} + O_{2(g)} \rightarrow CO_3^- + Ni^{3+} \qquad\qquad \text{Rxn(A2)}$$

$$CO_{(ads)} + CO_3^- + Ni^{3+} \rightarrow 2CO_{2(ads)} + Ni^{2+} \text{ (Slowest step)} \qquad\qquad \text{Rxn(A3)}$$

$$2CO_{2(ads)} \rightarrow 2CO_{2(g)} \qquad\qquad \text{Rxn(A4)}$$
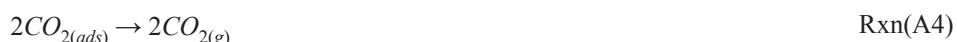
Now as per steady-state assumption for intermediate species $CO_{(ads)}$, one may obtain the below-given expression:

$$C_{CO(ads)} = \frac{k_{CO(g)} * C_{CO(g)}}{k_{O_2} * C_{Ni_2} * C_{O_2}} \qquad\qquad \text{(A1)}$$

Similarly, as per steady-state assumption for CO_3^- species, one may get the below expression:

$$C_{CO3^-} = \frac{k_{O_2} * C_{Ni^{2+}} * C_{O_2}}{k_{CO_2} * C_{Ni^{3+}}} \qquad\qquad \text{(A2)}$$

Since Rxn(A3) is the rate-determining step of the reaction, the surface deactivation (conversion of Ni^{3+} sites to Ni^{2+}) is controlled by Rxn(A3) and hence,

$$r_d = \frac{-da}{dt} = k_d * a^d * C_{CO3^-}^n * C_{CO(ads)}^m \qquad\qquad \text{(A3)}$$

Note that since initially the concentration of Ni^{3+} will be very high as compared to adsorbed CO molecules and CO_3^- (since we are using the catalyst in excess in the reactor), and also $C_{Ni^{3+}}$ is reported to remain constant.[7] Rxn(A3) being an elementary reaction (and hence n = stoichiometric coefficient = 1, m = stoichiometric coefficient = 1), and based on Eq(A1), Eq(A2) and followed by applying Pseudo steady-state assumption for Ni^{3+}, the final expression for deactivation of a catalyst can be given as below:

$$\frac{-da}{dt} = k_d'' * a^1 * C_{O_2}^1 * C_{CO_2}^2 \qquad\qquad \text{(A4)}$$

Here, since the catalyst deactivation is due to CO poisoning, it is generally observed that the order of deactivation 'd' is 1 and hence is allotted corresponding value.[17]